Received: 25 June 2023 | Revised: 10 January 2024 | Accepted: 20 February 2024

DOI: 10.1111/bph.16359

RESEARCH ARTICLE

BRD2-specific inhibitor, BBC0403, inhibits the progression of osteoarthritis pathogenesis in osteoarthritis-induced C57BL/6 male mice

Hyemi Lee[1] | Jiho Nam[1] | Hahyeong Jang[1] | Young-Sik Park[2] | Min-Hee Son[2] | In-Hyun Lee[2] | Seong-il Eyun[3] | Jae-Hyun Yang[4] | Jimin Jeon[1] | Siyoung Yang[1]

[1]Department of Biological Sciences, Sungkyunkwan University, Suwon, South Korea

[2]Benobio Co., Ltd, Seongnam, South Korea

[3]Department of Life Science, Chung-Ang University, Seoul, South Korea

[4]Paul F. Glenn Center for Biology of Aging Research, Department of Genetics, Blavatnik Institute Harvard Medical School (HMS), Boston, Massachusetts, USA

Correspondence
Siyoung Yang, Department of Biological Sciences, Sungkyunkwan University, Suwon 16419, South Korea.
Email: yangsy@skku.edu

Funding information
National Research Foundation, Grant/Award Numbers: NRF-2022R1A2C2004343, RS-2023-00223552, RS-2024-00400945, RS-2024-00335111

Background and Purpose: The discovery of new bromo- and extra-terminal inhibitors presents new drugs to treat osteoarthritis (OA).

Experimental Approach: The new drug, BBC0403, was identified in the DNA-encoded library screening system by searching for compounds that target BRD (bromodomain-containing) proteins. The binding force with BRD proteins was evaluated using time-resolved fluorescence energy transfer (TR-FRET) and binding kinetics assays. Subsequently, *in vitro* and *ex vivo* analyses demonstrated the effects of the BRD2 inhibitor, BBC0403, on OA. For animal experiments, medial meniscus destabilization was performed to create a 12-week-old male C57BL/6 mouse model, and intra-articular (i.a.) injections were administered. Histological and immunohistochemical analyses were then performed. The underlying mechanism was confirmed by gene set enrichment analysis (GSEA) using RNA-seq.

Key Results: TR-FRET and binding kinetics assays revealed that BBC0403 exhibited higher binding specificity for BRD2 compared to BRD3 and BRD4. The anti-OA effects of BBC0403 were tested at concentrations of 5, 10 and 20 μM (no cell toxicity in the range tested). The expression of catabolic factors, prostaglandin E2 (PGE_2) production and extracellular matrix (ECM) degradation was reduced. Additionally, the i.a. injection of BBC0403 prevented OA cartilage degradation in mice. Finally, BBC0403 was demonstrated to suppress NF-κB and MAPK signalling pathways.

Conclusion and Implications: This study demonstrated that BBC0403 is a novel BRD2-specific inhibitor and a potential i.a.-injectable therapeutic agent to treat OA.

KEYWORDS
BBC0403, BRD2, BRD2 inhibitor, intra-articular injection, osteoarthritis

Abbreviations: BBC0403, 2-(3,5-dimethyl-4-(oxetan-3-yloxy)phenyl)-5,7-dimethoxyquinazolin-4(3H)-one; BET, bromo- and extra-terminal; DEL, DNA-encoded chemical library; DMM, destabilization of the medial meniscus; ET, extra terminal; i.a., intra-articular; OA, osteoarthritis; SBP, subchondral bone plate.

1 | INTRODUCTION

Bromodomain-containing protein 2 (BRD2), a member of the protein family with both bromo- and extra-terminal (BET) domains, can be divided into three domains. These domains are referred to as the bromodomain 1 (BD1), bromodomain 2 (BD2) and an extra-terminal (ET) domain (Modukuri et al., 2022). Tandem bromodomains BD1 and BD2 are comprised of four alpha helices connected by two loops. These domains are members of the BET domain family. Both BD1 and BD2 can bind to acetylated lysine in target proteins and affect epigenetic regulation (Gilan et al., 2020). The structure of the ET domain comprises three alpha helices and one loop. The ET domain recruits effector proteins for regulatory functions (Wang, Shen, et al., 2021b).

BRD2 binds to acetylated histones and regulates gene expression, cell cycle progression and cell differentiation (Cheung et al., 2017; Shu et al., 2020; Wang, Wu, et al., 2021a). BRD2 is involved in the regulation of inflammatory gene expression and is implicated in the development of inflammatory diseases (Kang et al., 2023). BRD2 is vital for embryonic development (Shang et al., 2009).

Proteins with a BET domain, like BRD2, are called BET proteins. In addition to BRD2, the BET proteins include **BRD3**, **BRD4** and **BRDT**. BRD3 is involved in the cell cycle and is associated with cancer (Fu et al., 2015). BRD4 is closely related to transcription control and cell cycle progression. Similar to BRD3, it is associated with cancer and is a target for cancer treatment (Dong et al., 2018). BRDT is specifically expressed in the testes and plays an important role in spermatogenesis (Kohandani et al., 2022).

JQ1 is a small-molecule, multi-target inhibitor that targets BET proteins, including BRD2, BRD3, BRD4 and BRDT, which are involved in the regulation of gene expression (Belkina et al., 2013; Lockwood et al., 2012; Pinz et al., 2015; Shahbazi et al., 2016). Its function is to inhibit the binding of BET proteins to chromatin, leading to down-regulation of target genes. JQ1 has antitumor effects and has been studied as a potential therapeutic agent for other diseases, owing to its ability to modulate gene expression (Devaiah et al., 2016; Lovén et al., 2013; Ott et al., 2012). However, because JQ1 has the disadvantage of having a short half-life, it has not been tested in human clinical trials for its side effects (Wang, Wu, et al., 2021a; Yang et al., 2021).

Recently, a relationship between BRD3, BRD4 and **osteoarthritis (OA)** has been reported (An et al., 2018; Fukui et al., 2021; Jiang et al., 2017). OA, a degenerative joint disease, is one of the leading causes of impairment in senior citizens worldwide. Age is one of the most significant risk factors for developing OA. A sizeable majority of people may, at some time in their lives, experience discomfort linked to OA (Li et al., 2022). Cartilage destruction or defects on the articular cartilage surface can affect the subchondral bone or other tissues (Liao, Wang, et al., 2020a; Nagira et al., 2020; van der Poel et al., 2016).

Currently, symptom management is the only available treatment option for OA as there are no pharmaceuticals available that can prevent or slow the development of OA (Martel-Pelletier et al., 2016). This constitutes a critical aspect of modern research. One of the most popular options for relieving the discomfort caused by OA is the use of nonsteroidal anti-inflammatory drugs (NSAIDs). However, the substantial dose-dependent side effects of NSAIDs have led specialists to advise patients against the recommended daily administration (da Costa et al., 2017). Indigestion, stomach pain, nausea and diarrhoea are possible side effects that may result in stomach ulcers, anaemia and intestinal bleeding (McGettigan & Henry, 2013).

Direct access to the joint space provided by intra-articular (i.a.) medication delivery improves the bioavailability of therapeutic medicines at the affected location, decreases systemic exposure and lowers total cost (Li et al., 2021). Currently, OA is routinely treated with i.a. injections; however, few treatment options exist for i.a. treatment. Corticosteroids are mainly used to alleviate OA-related pain and resolve joint effusion with i.a. injection but not oral administration. (Ayhan et al., 2014). Although these treatments may temporarily improve symptoms, they do not alter disease progression. **Hyaluronic acid**, a visco-supplement approved by the Food and Drug Administration (FDA), is widely used to treat OA. However, there is no evidence that hyaluronic acid in its current form can prevent or delay the need for joint replacement (Jørgensen et al., 2010). An ideal i.a. drug delivery platform must have a disease-modifying effect on cartilage regeneration, have no or minimal safety concerns and offer controlled release of the therapeutic agent with extended bioavailability and joint retention. Recent progress in this area has not resulted in the development of a single i.a. drug-delivery platform that satisfies all these criteria. However, the specific inhibition of BRD2 is strongly indicated to satisfy the criteria mentioned above. Animals are biologically similar to humans. Mice share more than 98% of the human DNA. Animals can develop cancer, diabetes and heart disease.

What is already known

- For osteoarthritis (OA) there are no available medications that can prevent or delay its beginning.
- BRD2 plays a major role in controlling the expression of genes related to inflammation.

What does this study add

- The intra-articular injection of BBC0403 halted cartilage of knee joint degradation in mice with osteoarthritis.
- BBC0403 was shown to inhibit the NF-κB and MAPK signalling pathways.

What is the clinical significance

- BBC0403, a new specific BRD2 inhibitor is a potential therapeutic agent for the treatment OA.

Animal models, which have shorter life cycles than humans, can be studied throughout their lifespan and through generations, facilitating the generation of the knowledge essential for understanding disease processes and how they interact with living biological systems (Kiani et al., 2022; Leong et al., 2015). Based on the present study we suggest that BBC0403 (2-(3,5-dimethyl-4-(oxetan-3-yloxy)phenyl)-5,7-dimethoxyquinazolin-4(3H)-one), a specific BRD2 inhibitor, is a strong candidate for developing i.a. medications in a 12-week-old C57BL/6 male mouse model.

2 | METHODS

2.1 | Screening of DNA-encoded chemical library (DEL) with bromodomains from BRD2, BRD3 and BRD4

Novel bromo- and extra-terminal domain inhibitors (BETi) were identified by screening a DEL (WuXi AppTec, Shanghai, China) with BD1s and BD2s from BRD2, BRD3 and BRD4 proteins. These proteins were generated by amplifying the relevant sections of the BRD2- to BRD4-encoding genes, placing the sections into pET28a vectors (Novagen, Northumberland, UK), transforming *Escherichia coli* BL21 (DE3) (Novagen) with each plasmid and inducing protein expression by treatment with 0.2-mM isopropyl β-D-thiogalactopyranoside for 16 h at 18°C. The bacteria were collected, resuspended in a lysis buffer (50-mM Tris [pH 8.2] (Thermo Fisher scientific, MA, USA), 300-mM NaCl (LPS solution, Daejeon, South Korea) and 20-mM imidazole (Sigma, MO, USA) and sonicated. The lysates were centrifuged at 1550 × *g* for 1 h at 4 °C, after which the supernatant was loaded onto a nickel affinity HisTrap HP column (GE Healthcare, Chicago, IL, USA). After washing the column, BRD2, BRD3 and BRD4 were eluted with 50-mM Tris buffer (pH 8.2) containing 300-mM NaCl and 500-mM imidazole.

2.2 | Time-resolved fluorescence resonance energy transfer (TR-FRET) assay

TR-FRET assay kits from BPS Bioscience (BPS Bioscience, CA, USA) that were specific for BRD2 (BD1 + BD2), BRD3 (BD1 + BD2) and BRD4 (BD1 + BD2) were used. The BD ligands were diluted with water. Master mixes consisting of 1× BRD homogeneous assay buffer and diluted BD ligands were prepared. BRD proteins were thawed on ice and diluted with 1× BRD homogeneous assay buffer. Subsequently, 1.5 µl of the master mix was added to each well of a microplate (Labcyte, CA, USA), and reactions were initiated by adding 5 µl of diluted BRD protein to each well. The plates were then incubated at 20°C–22°C for 30–60 min. GSH acceptor beads (Perkin Elmer, MA, USA) and streptavidin-conjugated donor beads (Perkin Elmer) were diluted with 1× BRD homogeneous detection buffer 1. Then, 10 µl of acceptor bead mixture was added to each well. After incubation at 18°C for 30 min, 10 µl of donor bead mixture was added to each well, followed by incubation at 18°C for 15–30 min. Alpha-particle counts were determined using an EnVision 2105 multimode plate reader (Perkin Elmer).

2.3 | Binding kinetics assay

Binding kinetic analysis was performed using the Sartorius Octet® R2 system (Sartorius, Gottingen, Germany). Superstreptavidin biosensors were loaded with biotinylated BRD2 BD1, BRD2 BD2, BRD3 BD1, BRD3 BD2 BRD4 BD1, BRD4 BD2 or biotin as a control in phosphate-buffered saline with Tween 20 buffer (PBST) (PBS (LPS solution), 0.02% Tween 20 (LPS solution), 5% DMSO (Sigma)) and dipped into the compound solution for 10 min. The binding of the compound to proteins was tested by dipping an individual sensor into a series of protein dilutions for 180 s to measure binding (kon) and into blank buffer PBST to measure the off rate (koff). Simultaneously, another compound sensor was dipped into a blank buffer, PBST, to serve as a control. Competition binding assays were performed by dipping the compound sensor in a mixture of proteins and testing chemicals.

2.4 | Pharmacokinetics (PK) analysis of BBC0403

SD-rats (male, 6-week-old) were obtained from Orient Bio (Seoul, Korea) and housed under pathogen-free conditions. Animal care was performed following the guidelines of the Animal Care Facility at Biotoxtech Co. Ltd. (Chungcheong Buk-Do, Korea). The rats were housed in standard laboratory cages with 1 rat per cage. They were provided with standard chow and water ad libitum. The temperature in the housing facility was maintained at 23°C. The rats were euthanized using CO2, and to ensure that they were dead, permanent cessation of circulation was confirmed. Animal studies are reported in compliance with the ARRIVE guidelines (Percie du Sert et al., 2020) and with the recommendations made by the *British Journal of Pharmacology* (Lilley et al., 2020).

SD rats were intravenously injected with BBC0403 (5 or 25 $mg \cdot kg^{-1}$) to determine the pharmacokinetics of BBC0403. Blood sampling was conducted while the subject was under general anaesthesia, administered through an intraperitoneal injection of ketamine (80 $mg \cdot kg^{-1}$) and xylazine (10 $mg \cdot kg^{-1}$). The anesthesia depth was monitored continuously by observing vital signs such as heart rate, respiratory rate, body temperature and the pedal reflex. A local anaesthetic cream was also applied to the sampling site 30 min prior to the procedure. To begin, the sternal area of the rat's collarbone was disinfected with alcohol, and a pulse was checked for. Following this, a 25G needle, pointing upwards, was inserted into the collarbone area. The syringe was gently manipulated to ensure efficient blood draw into the needle, before proceeding with the blood collection. Afterward, a piece of cotton was applied to the puncture site to manage any bleeding. Blood samples were collected from the jugular vein at various intervals, mixed with 3.8% (w/v) sodium citrate (Sigma) and

centrifuged at 8000 × *g* for 30 min to obtain plasma. The rat plasma samples were then mixed with acetonitrile (33%, v/v) (Sigma), vortexed for 5 min and centrifuged at 13,000 × *g* for 10 min. The concentration of BBC0403 in plasma was determined by HPLC (Shimadzu, Japan) with a UV detector. Pharmacokinetic parameters were analysed using Microsoft Excel (Sato et al., 1996).

2.5 | Cell and reagent for treatment

According to a previous study (Jeon et al., 2023), primary mouse cells that were used for the *in vitro* tests were primary mouse chondrocytes, and they were taken from ICR mice that were 5 days old (DBL, Chungbuk, South Korea).

The Institutional Animal Care and Use Committee (IACUC) of Sungkyunkwan University approved the planned animal experiments. We created several experimental conditions to observe the anti-catabolic effects of BBC0403 on chondrocytes. First, chondrocytes were treated with BBD0403 at concentrations of 5, 10 and 20 μM for 12 h, with 1 ng·ml^{-1} **IL-1β** recombinant protein as a negative control and JQ1 (thienotriazolodiazepine, a potent inhibitor of the BET family) (Sigma) as a positive control. Second, BBC0403 was treated at the above concentrations for 12 h in a medium containing interleukin (IL)-1β, and a portion was harvested. Additionally, only cells treated with high concentrations of BBC0403 were replaced with IL-1β-only medium and cultured for an additional 12 h. Finally, after culturing for 12 h in a medium containing IL-1β, BBC0403 was added at various concentrations without changing the medium. Control samples were treated with PBS (**LPS** solution; Daejeon, South Korea).

2.6 | LDH assay

Cartilage explants were taken from the knee joints of 5-day-old mice to isolate chondrocytes. A 96-well plate was used to grow the cells (1×10^4 cells per well). After 12 h, cell survival was determined using a LDH colorimetric assay kit (BioVision, MA, USA) as described previously (Lee et al., 2020). Samples with 100% and 0% viability after treatment with Triton X-100 were used for normalization. The supernatants of chondrocytes incubated with BBC0403 at various doses for 12 h were analysed. The percentage of viable cells was determined using the following equation: % of viable cells = 100 − (sample LDH − negative control)/(max LDH − negative control) × 100. All signals were read at 495 nm using a SYNERGY H1 microplate reader (BioTek, Vermont, USA).

2.7 | RT-PCR and quantitative RT-PCR (qRT-PCR)

As described previously, total RNA was extracted from mouse articular chondrocytes, and reverse transcription was used to generate cDNA. Primers utilized in the PCR were as follows: mouse Mmp3 (5′-TCCTGATGTTGGTGGCTTCAG-3′ and 5′-TGTCTTGGCAAATCC GGTGTA-3′); mouse Mmp13 (5′-TGATGGACCTTCTGGTCTTCTGG-3′ and 5′-CATCCACATGGTTGGGAAGTTCT-3′); mouse Cox2 (5′-GGTCTGGTGCCTGGTCTGATGAT-3′ and 5′-GTCCTTTCAAGGAGA-ATGGTGC-3′); mouse Il-6 (5′-ACCACTCCCAACAGACCTGTCTATA CC-3′ and 5′-CTCCTTCTGTGACTCCAGCTTATCTGTTAG-3′). The mouse glyceraldehyde quantification of gene transcript levels was accomplished by qRT-PCR using SYBR premix ExTaq (Takara Bio, Shiga, Japan), normalized to Gapdh level.

2.8 | Protein isolation and western blotting

As previously described (Jeon et al., 2023), chondrocyte proteins were extracted using a lysis buffer (150-mM NaMCl, 1% NP-40 (Millipore, MA, USA), 50-mM Tris, 0.2% sodium dodecyl sulphate and 5-mM NaF) containing protease and phosphatase inhibitors. **COX-2** and **ERK** were isolated from chondrocytes. **MMP3** and **MMP13** were isolated from the media. Trichloroacetic acid (TCA) precipitation isolates secreted MMP3 and MMP13 TCA-precipitated proteins from the conditioned media. In addition, TCA (Sigma) was removed from the protein pellet by centrifugation of the supernatant and adding 1-ml acetone in the tube. Anti-MMP3 (ab52915; Abcam, Cambridge, UK, RRID:AB_881243), anti-MMP13 (ab39012; Abcam, RRID:AB_776416), anti-COX2 (ab52237; Abcam, RRID:AB_869240), anti-ERK1/2 (sc-514302; Santa Cruz Biotechnology, Santa Cruz, TX, USA, RRID:AB_2571739) and anti-pERK, **JNK**, pJNK, **p38**, pp38, p65 and pp65 (9101S, 9252S, 9251S, 9212S, 9215S, 8242S, 3033S; Cell Signaling Technology, Beverly, WA, USA) antibodies were employed after western blot. Anti-ERK1/2 antibodies were used to measure the protein levels (Cho et al., 2023; Jeon et al., 2023). Densitometric analysis (AlphaEase FC 4.0; Alpha Innotech, San Leandro, CA, USA) was used to adjust the band intensities according to ERK intensity.

2.9 | Destabilization of the medial meniscus (DMM) surgery and i.a. injection

Male C57BL/6 mice (12 weeks old) weighing 18–20 g were obtained from DBL (Chungbuk, South Korea) and maintained under regulated environmental conditions. The mice were housed in groups of four per cage, maintained at a temperature of 23°C and subjected to a 12-h light/dark cycle. Unrestricted amounts of food and water were provided.

The IACUC of Sungkyunkwan University approved all the experiments. C57BL/6 male mice (12-week-old) were used to establish the OA mouse model. C57BL/6 male mice are commonly used because of the ease of breeding and availability of congenic strains; their robustness and OA are affected by sex hormones. When DMM surgery was performed, male mice showed higher OA severity than female mice. Ovariectomized female mice also showed higher OA severity than control females (Ma et al., 2007). Before DMM surgery, all animals were anaesthetized using 100 mg·kg^{-1} ketamine (Yuhan Corporation,

Seoul, South Korea) and 5 mg·kg^{-1} xylazine (Elanco, Ansan, South Korea) administered intraperitoneally following the Cold Spring Harbor Protocols. Mice were allowed to breathe spontaneously and were placed on blanket to maintain body temperature. Medial meniscal instability is achieved via the transection of the medial meniscotibial ligament during DMM. As reported previously (Jeon et al., 2023), cartilage destruction in the femur can be detected 12 weeks after DMM surgery. In this study, we induced OA during DMM surgery for 10 weeks. The DMM usually damages the cartilage's medial side by cutting the medial meniscotibial ligament (Glasson et al., 2007). Ten-week-old C57BL/6 male mice were subjected to DMM following a previously described method (Jeon et al., 2023). Four weeks after surgery, BBC0403 was injected i.a. once per week. The sham group did not undergo the DMM surgery. The control group underwent DMM surgery with PBS. Ten weeks after the DMM surgery, the mice were killed for histopathological analysis.

2.10 | Explant culture and alcian blue staining

Cartilages isolated from ICR mice (5 days old) were cultured in DMEM for 24 h and were treated with **IL-1β** and BBC0403 for 24 h. Cartilage was fixed in 4% paraformaldehyde and dehydrated using a gradient of ethanol and xylene. Finally, the cartilage samples were transferred to a paraffin block. Paraffin blocks were sectioned with a thickness of 5 μm. Paraffin was substituted with xylene, and cartilage sections were dehydrated using a gradient ethanol. Alcian blue 1% solution (pH 2.5) was made using 0.1-N HCl and alcian blue 8GX (A9186-10G; MiliporeSigma, MA, USA); sections were stained with alcian blue solution for 10 min at 25°C. The sections were de-stained using 0.1-N HCL and washed with deionized water.

2.11 | Safranin O staining and immunohistochemistry (IHC)

As previously described, the histopathological examination involved Safranin O (Sigma) staining (Cho et al., 2023). Knee joints isolated from sacrificed mice were fixed in paraformaldehyde and decalcified with EDTA for 2 weeks. Knee joints were placed in paraffin blocks and dehydrated using an ethanol and xylene gradient. Paraffin blocks were serially cut into 5-μm-thick sections using a microtome. Sections were deparaffinized using xylene substitution and an ethanol gradient and hydrated before staining with Safranin O. The stained knee joint slices were examined using the Osteoarthritis Research Society International (OARSI) grading system; subchondral bone plate (SBP) thickness was measured to determine the extent of cartilage damage (Jeon et al., 2023). Specially, SBP thickness was measured as the average length obtained from three different sections to assess subchondral bone sclerosis using an Aperio Image Scope (Leica Biosystems, IL, USA) (Nagira et al., 2020). Two investigators scored all the histology samples in a blinded and independent manner. Immunohistochemistry was used to determine protein expression in chondrocytes from the cartilage. The intensity of immunohistochemistry (IHC) staining was normalized to the number of cells in the field of view. The hydration process resembled that used in Safranin O staining. Primary antibodies against IgG (#10500C; Invitrogen, MA, USA, RRID:AB_2532981), 8-Hydroxyguanosine (8-OHdG; GTX41980; GeneTex, CA, USA), MMP3 (ab52915; Abcam, RRID:AB_881243), MMP13 (ab39012; Abcam, RRID:AB_776416) and COX2 (ab52237; Abcam, RRID:AB_869240) (Jeon et al., 2023) were applied to the samples. Finally, the samples were visualized using aminoethyl carbazole before quantification using ImageJ software. The Immuno-related procedures used comply with the recommendations made by the *British Journal of Pharmacology* (Alexander et al., 2018)

2.12 | Data and statistical analysis

The data and statistical analysis comply with the recommendations of the *British Journal of Pharmacology* on experimental design and analysis in pharmacology (Curtis et al., 2022). Statistical analyses were conducted by initially employing the Shapiro–Wilk test to assess normality. Because all data were from three or more groups, one-way ANOVA using the Bonferroni post hoc test was applied for normally distributed data, and the Kruskal–Wallis test using Dunn's test was applied for nonparametric data. Post hoc tests were conducted only if F in ANOVA achieved $P < 0.05$. Results are presented as the mean ± SD. All histological samples were scored blindly and independently by two investigators. P values < 0.05 are marked with an asterisk (*), indicating statistical significance. Statistical analysis was performed using the group size given by the number of independent values. All experiments used for statistical analysis were performed at least five times for each group ($n = 5$, where n refers to the number of independent data points). The number of independent values is provided in the figure legends (biological replicates, not technical replicates), and statistical analyses were performed using these independent values. The Statistical Software GraphPad Prism 7 was used for the analysis (GraphPad, San Diego, CA, USA). This study followed the editorial guidelines on experimental design andanalysis in pharmacology (Curtis et al., 2022).

2.13 | Materials

BBC0403 (2-(3,5-dimethyl-4-(oxetan-3-yloxy)phenyl)-5,7-dimethoxyquinazolin-4(3H)-one) was synthesised in Benobio Co (Seongnam, South Korea). (Please contact Siyoung Yang, Department of Biological Sciences, Sungkyunkwan University, Suwon 16419, South Korea. Email:yangsy@skku.edu for details of synthesis and supply). Isopropyl β-D-thiogalactopyranoside was purchase from Sigma, (MO, USA) while IL-1βand IL-1β recombinant protein was obtained purchased GenScript Biotech (Piscataway, NJ, USA). Sodium dodecyl protease and phosphatase inhibitors were purchased from Roche (Basel, Switzerland), while alcian blue 8GX (A9186-10G;) was purchased from MiliporeSigma (MA, USA) and LPS solution was purchased from

Daejeon, (South Korea). Details of other materials and suppliers were provided in the specific sections

2.14 | Nomenclature of targets and ligands

Key protein targets and ligands in this article are hyperlinked to corresponding entries in the IUPHAR/BPS Guide to PHARMACOLOGY http://www.guidetopharmacology.org and are permanently archived in the Concise Guide to PHARMACOLOGY 2023/24 (Alexander, Fabbro, Kelly et al., 2023a,b)

3 | RESULTS

3.1 | BBC0403 showed specific binding to BRD2

Molecules targeting BD1 and BD2 domains of BRD2–4 were screened using the WUXI DEL (Figure 1a). BBC0403 was selected as the small-molecule inhibitor (Figure 1b). It was synthesized and confirmed to exhibit high binding specificity to BRD2 compared to BRD3 and BRD4, as demonstrated by its TR-FRET and KD values (Figure 1c–f). Pharmacokinetic profiles were analysed after intravenous injection of BBC0403; pharmacokinetic parameters, including Cmax, half-life and AUC, are shown in Figure 1g. The time required to metabolize and eliminate BBC0403 from the bloodstream increased in a dose-dependent manner.

The cytotoxicity of BBC0403 was evaluated in mouse primary chondrocytes *in vitro*. The LDH assay results demonstrated that the cell viability of BBC0403 did not exhibit variations within the range of 0.5–20 μM, but not 50 μM, when compared to the control group at 0 μM (Figure S1A), indicating that within this range, BBC0403 exhibited no adverse effects on cell survival. Therefore, the *in vitro* experiments were performed within the 0.5–20 μM concentration range. Fibroblast-like synoviocytes (FLS) are found in synovial tissues and are the primary cellular constituents of the synovium in joints. In addition, the cytotoxicity of BBC0403 against fibroblast-like synoviocytes cells was confirmed using the same concentration range used for chondrocytes; no effect on cell viability was noted (Figure S1B).

3.2 | BBC0403 suppressed the expression of OA-inducing genes in the presence of IL-1β

BBC0403, a new BRD2 inhibitor, was tested for its anti-catabolic effect at 5, 10 and 20 μM concentrations, at which the chondrocytes viability did not show any significant differences compared to the control group with 0-μM concentration. IL-1β was co-administered to mimic OA-like conditions by increasing the expression of Mmp3, Mmp13, Cox2 and Il-6, catabolic factors that degrade cartilage or are associated with inflammation. In mouse primary chondrocytes treated with BBC0403 and IL-1β, BBC0403 inhibited the expression of catabolic factors. RT-PCR and qRT-PCR confirmed the anti-catabolic effects of BBC0403 on mRNA levels; its effects on protein levels were confirmed by western blotting (Figure 2a–d).

As previously reported, Cox2 tissue-specific knockout mice do not produce prostaglandin E_2 (PGE_2). PGE_2 production involves Cox2 and is activated in OA cartilage (Akhtar & Haqqi, 2012). In the culture medium where chondrocytes were cultured, BBC0403 reduced PGE_2 production that induced IL-1β (Figure 2e). The levels of pro-inflammatory cytokines were measured. Various pro-inflammatory cytokines are secreted under OA conditions (Kapoor et al., 2011). The level of IL-6 was evaluated by ELISA in culture supernatant obtained after cotreating IL-1β and BBC0403. The level of IL-6 protein was also decreased by BBC0403 treatment compared with the group treated with IL-1β only (Figure 2f).

We further confirmed that the anti-catabolic effects of BBC0403 were sustained. The chondrocytes were co-treated with BBC0403 and IL-1β for 12 h and then incubated for another 12 h with IL-1β (Figure S2A). Although these chondrocytes were stimulated with IL-1β for the last 12 h without BBC0403, catabolic factors were decreased by pretreatment with BBC0403 (Figure S2B). These data suggest that the anti-catabolic effect of BBC0403 was sustained.

Gene set enrichment analysis was conducted on OA-related genes to analyse the RNA-seq data for BBC0403. A list of 269 OA-related genes was obtained using Ingenuity Pathways Analysis (IPA). Down-regulated genes in OA are associated with matrix degradation, inflammation and ROS production. According to the gene set enrichment analysis results (Figure 2g), BBC0403 down-regulated Mmp3, Mmp13, Cox2, Il-6 and ROS production associated with OA's cartilage destruction.

The anti-extracellular matrix (ECM) degradation effects of BBC0403 were confirmed in *ex vivo* experiments using cartilage explants. When cartilage explants were stained by alcian blue, a cationic dye binding to sulfated glycosaminoglycans, cartilage explant co-treated with BBC0403 with IL-1β was dyed dark compared to IL-1β (Figure 2h).

Before checking the *in vivo* effect of BBC0403, we first checked the *in vitro* OA mimic conditions with IL-1β treatment for 24 h. Chondrocytes were treated with BBC0403 for 12 h after IL-1β pretreatment for 12 h (Figure S2D) to make *in vitro* mimic OA conditions. Although IL-1β increased catabolic factor expression, BBC0403 could inhibit IL-1β induced catabolic factor expression (Figure S2E,F). Thus, BBC0403 may be a strong therapeutic agent for suppressing the expression of catabolic factors and inhibiting cartilage destruction in vivo.

3.3 | Intra-articular (i.a) injection of BBC0403 prevented OA cartilage degradation

As previously stated, BBC0403 decreased IL-1β-induced expression of catabolic factors in mouse primary chondrocytes. *In vivo* experiments were conducted using 12-week-old C57BL/6 male mice to determine whether the anti-OA effects of BBC0403 would be

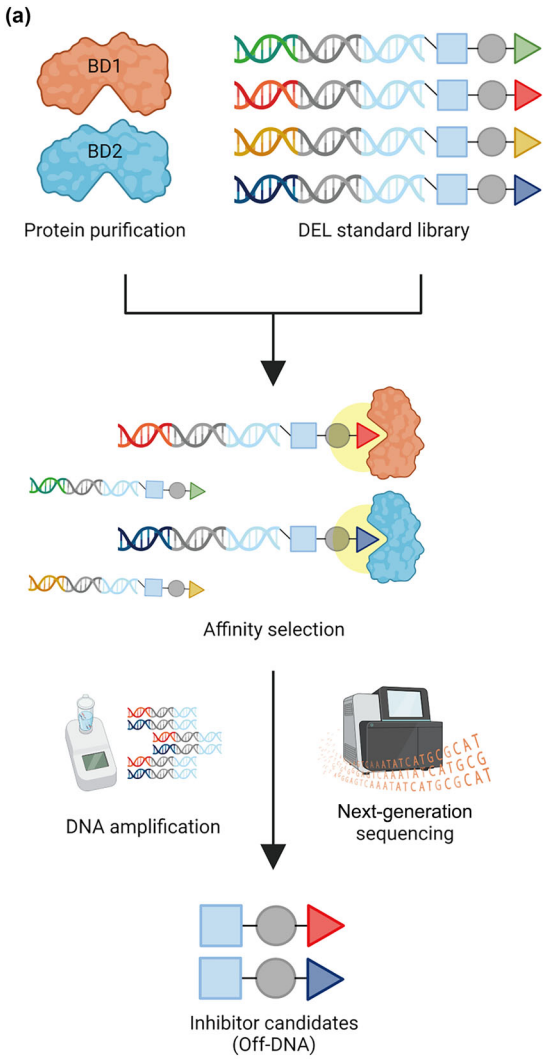

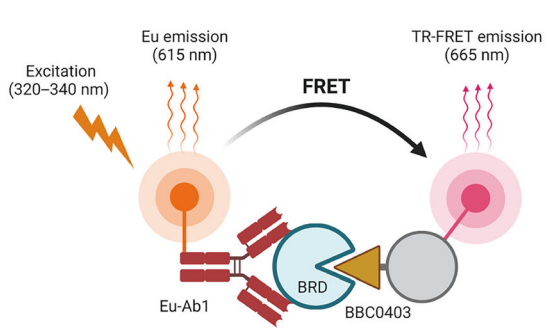

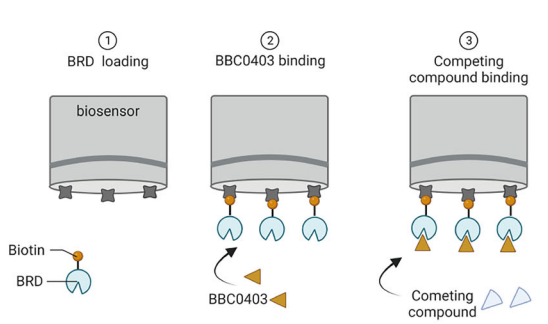

(e)

BBC0403	BRD protein		
	BRD2	BRD3	BRD4
TR-FRET value (RLU)	43130	>100,000	>100,000

(f)

BBC0403	BRD protein					
	BRD2 (BD1)	BRD2 (BD2)	BRD3 (BD1)	BRD3 (BD2)	BRD4 (BD1)	BRD4 (BD2)
Kd value (μM)	41.37	7.64	>1000	-	>1000	>1000

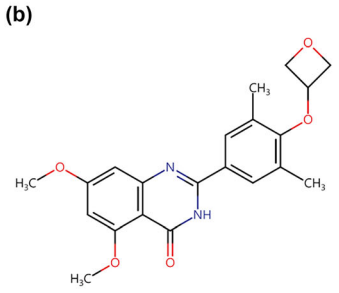

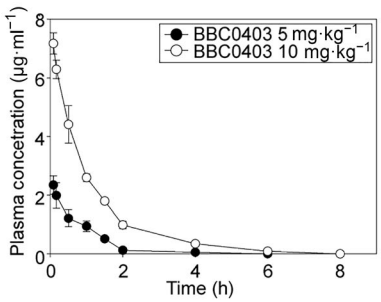

BBC0403	5 mg·kg^{-1}	25 mg·kg^{-1}
Cmax (μg·ml^{-1})	2.343	7.178
Half-life (h)	0.61	0.95
AUC0-t (μg·h·ml^{-1})	2.01	7.874

FIGURE 1 BBC0403 is bound to BRD2 more strongly than BRD3 and 4. (a) Scheme of DNA-encoded chemical library (DEL) screening. Purified target proteins and the DEL standard library were needed for DEL screening. The DNA was amplified after selecting a DNA-encoded chemical compound that binds to the target protein by mixing the two. Next-generation sequencing was conducted to find a candidate chemical for inhibition. (b) BBC0403 (2-(3,5-dimethyl-4-(oxetan-3-yloxy)phenyl)-5,7-dimethoxyquinazolin-4(3H)-one) structure. (c, d) Scheme and value of TR-FRET assay. Among the BRD proteins, the stronger the binding force with BBC0403, the lower the TR-FRET value because it cannot bind to the BD ligand. (e, f) Scheme and value of binding kinetics assay. A binding kinetics assay using a biosensor was performed to compare the binding force of BBC0403 with the domains of each protein. The KD value is a dissociation constant value, the smaller the value, the stronger the coupling force. (g) Concentration in plasma was measured after i.v. injection of 5 and 25 mg·kg^{-1} to evaluate long-term biocompatibility. The pharmacokinetic parameter of BBC0403 following i.v. injection in normal rats. Cmax is the maximum observed plasma concentration.

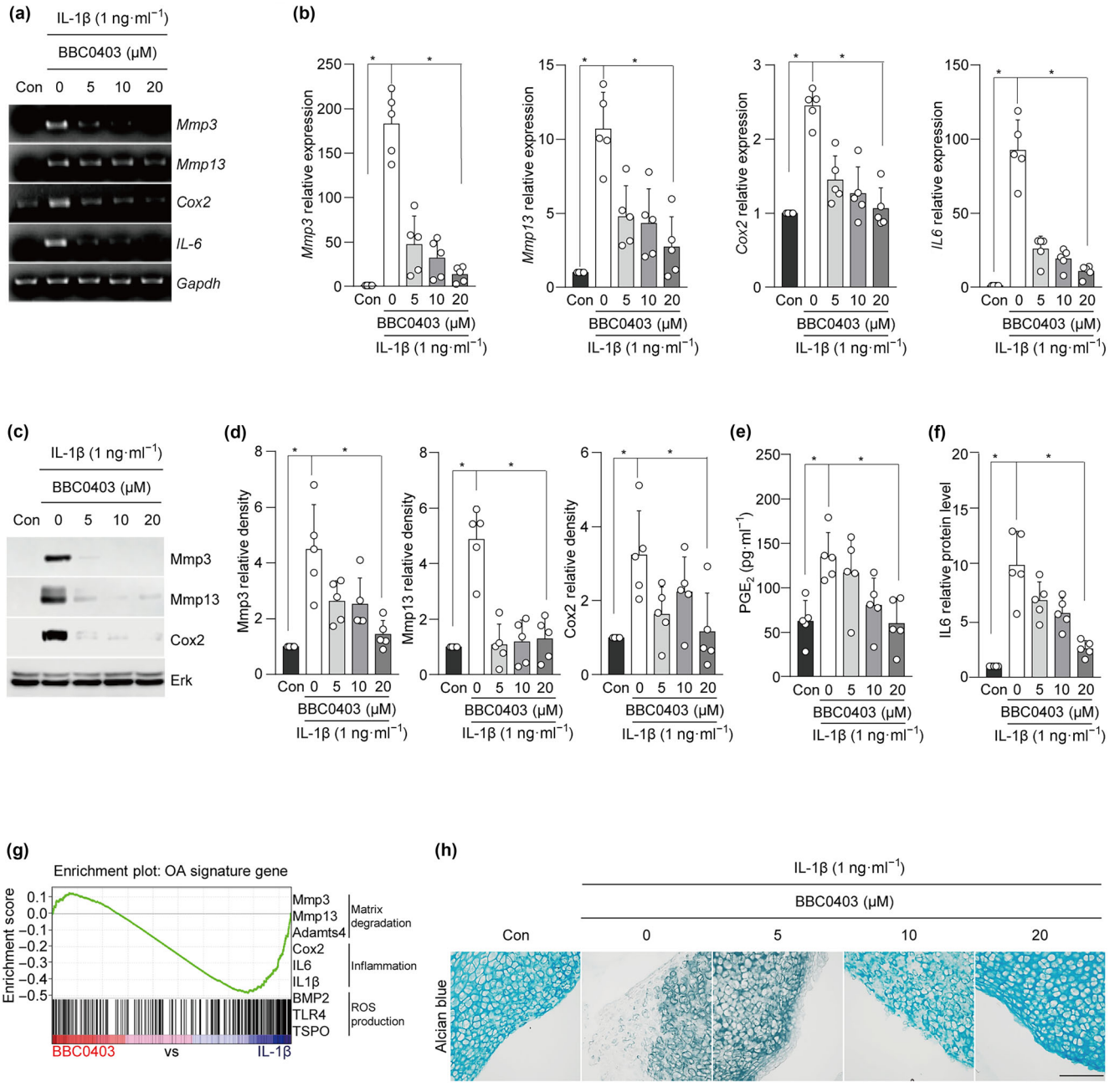

FIGURE 2 BBC0403 decreased catabolic factors in osteoarthritis (OA) mimic condition and inhibited extracellular matrix (ECM) degradation. (a–f) BBC0403 at various concentrations and IL-1β (1 ng·ml^{-1}) were applied for 12 h to mouse articular chondrocytes to show the anti-catabolic effect of BBC0403 *in vitro*. The levels of Mmp3, Mmp13, Cox2 and Il-6 were evaluated by PCR (a), qRT-PCR (b), western blotting (c) and densitometry (n = 5) (d). Glyceraldehyde-3-phosphate dehydrogenase (GAPDH) and ERK concentrations were used to normalize each gene and protein level. (e) The level of PGE_2 in the culture media was analysed by ELISA (n = 5). (f) The protein level of IL-6 in the culture supernatant was analysed by ELISA (n = 5). (g) Gene set enrichment analysis (GSEA) was conducted using RNA-seq data gained from chondrocytes. (h) The alcian blue solution-stained cartilage explants. Each explant acquired from a 5-day-old mouse was treated with BBC0403 and IL-1β (1 ng·ml^{-1}) for 72 h. The explant was imaged under the microscope at 400×. Scale bar = 100 μm. Values are presented as means ± SD and were assessed using one-way ANOVA with Bonferroni's test (e) and Kruskal–Wallis test using Dunn's test (b, d, f). *P < 0.05. Control: The group treated with PBS was the control.

confirmed in a mouse model. The DMM surgery, which destabilizes the medial meniscus by transecting the medial meniscotibial ligament, is a representative method for creating an OA mouse model. We performed DMM surgery on C57BL/6 mice. Furthermore, all OA therapeutic agents were used onset of or after cartilage destruction (Zhang et al., 2019). The time point of OA development should be selected to determine the exact therapeutic effect of BBC0403. One advantage of the DMM model is that it makes it possible to monitor

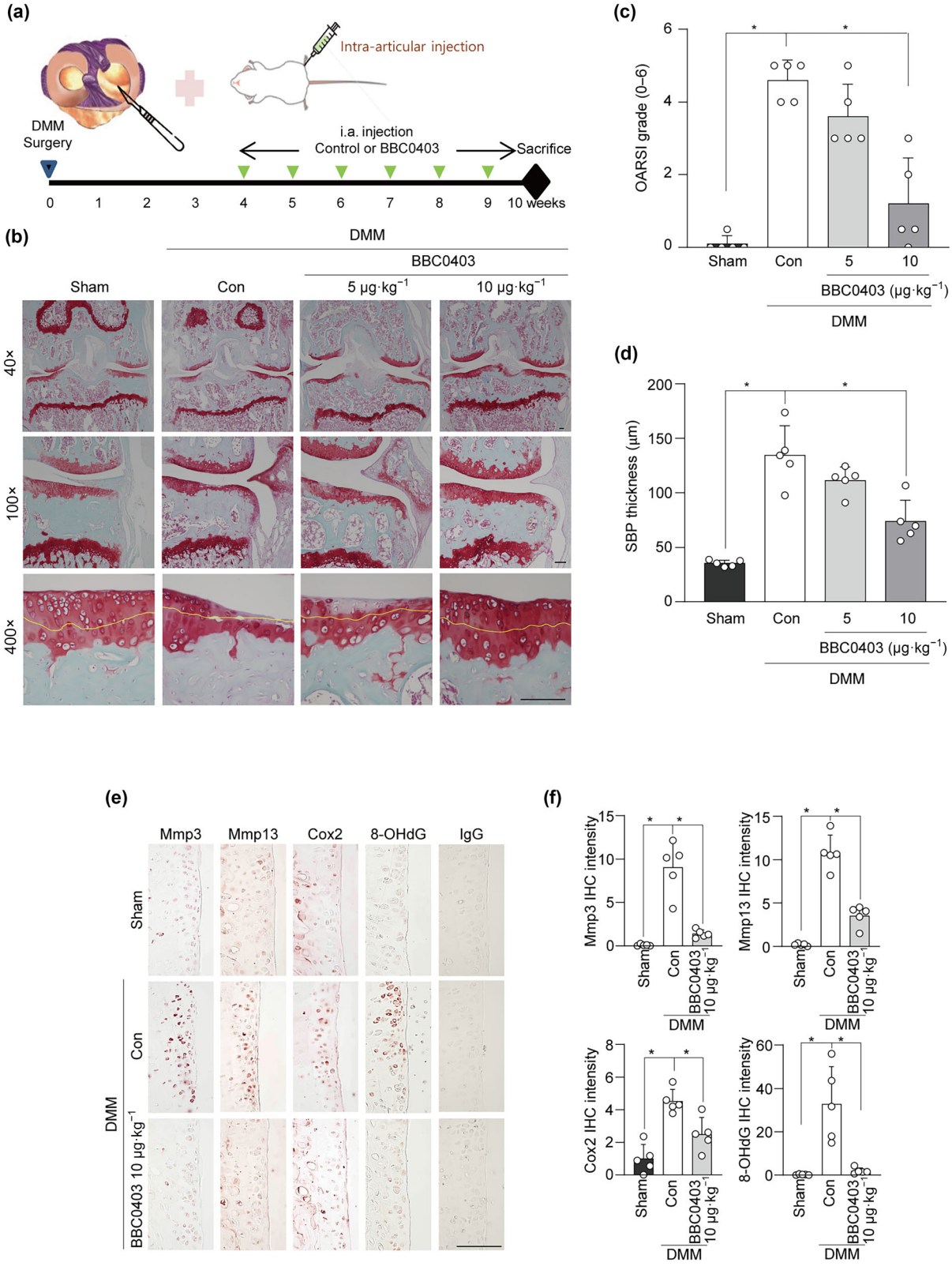

FIGURE 3 Legend on next page.

the onset of cartilage destruction; cartilage destruction begins to increase gradually 4 weeks after DMM surgery (Jeon et al., 2023).

For 4–10 weeks after DMM surgery, BBC0403 was injected by i.a. once a week. The mice were euthanized 10 weeks after the DMM surgery (Figure 3a), and tissues were analysed. When 10 $\mu g \cdot kg^{-1}$ BBC0403 was injected after DMM surgery, cartilage destruction was prevented, compared to the PBS control where cartilage destruction occurred (Figure 3b). I.a. injection of BBC0403 inhibited DMM-induced OA manifestations in an injection time-dependent manner (Figure S3). We applied the Osteoarthritis Research Society International grading system to evaluate the severity of OA, particularly in the knees (Glasson et al., 2010). subchondral bone plate (SBP) thickness is related to the bone structure beneath the articular cartilage of the joints. Changes in SBP thickness are associated with OA. The correlation between the Osteoarthritis Research Society International grade and SBP thickness lies in its correlation with OA progression and severity. In OA, changes occur not only in the cartilage but also in the underlying bone. The subchondral bone undergoes remodelling and becomes capable of affecting SBP thickness. The relationship between Osteoarthritis Research Society International grade and SBP thickness can provide insights into the extent of joint degeneration and the pathological changes occurring in OA (Nagira et al., 2020). We next checked the Osteoarthritis Research Society International grade and SBP thickness and found that they were also decreased by i.a. injection of BBC0403 (Figure 3c,d). These results indicate that BBC0403 inhibits cartilage degradation and OA progression. Additionally, immunohistochemistry was conducted on a section of the mouse knee joint to confirm protein changes. When BBC0403 was injected into the knee joint of a mouse undergoing DMM surgery, the protein levels of Mmp3, Mmp13 and Cox2 decreased. The expression level of 8-hydroxyguanosine (8-OHdG), a biomarker used to assess ROS generation, was measured in mouse cartilage. This effect originates from the oxidation of DNA by ROS. Immunohistochemistry demonstrated that BBC0403 prevented ROS generation in the cartilage of mice injected with BBC0403-i.a. after DMM surgery (Figure 3e,f). Furthermore, we did not detect any organ cytotoxicity, such as in the liver, lungs or synovium (Figure S4). Based on these findings, BBC0403 appears to be a viable therapeutic agent for treating OA via i.a. injection without any *in vivo* cytotoxicity.

In addition to DMM surgery, monoiodoacetate (MIA) injection is used to create acute OA animal models and to induce rapid cartilage destruction. Owing to its short induction period, it cannot accurately determine the time point at which OA breaks out (Miyamoto et al., 2016; Sampath et al., 2021). The onset of OA symptoms, such as the time point of cartilage destruction or pain induction, should be considered for the development of therapeutic agents. It is difficult to induce OA symptoms in the monoiodoacetate (MIA) mouse model but not in the DMM-induced model (Cho et al., 2022; Jeon et al., 2023). We performed an MIA mimic *in vitro* analysis to prove that the BRD2 inhibitor BBC0403 is suitable for inhibiting the development of acute OA. MIA inhibits Krebs cycle, resulting in cell death (Kuyinu et al., 2016). H_2O_2 treatment showed similar molecular mechanisms *in vitro* (Yoo et al., 2022). We performed an LDH assay after treating chondrocytes with H_2O_2 and assessed chondrocyte death. The results demonstrated that BBC0403, a specific BRD2 inhibitor, suppressed H_2O_2-induced cell death (Figure S5), indicating that BBC0403 protects against the development of acute OA.

3.4 | BBC0403 prevented OA by inhibiting NF-κB and MAPK signalling

We focused on the changes in gene expression associated with NF-κB and MAPK signalling to elucidate how BBC0403 prevents OA. In general, lists of genes can be analysed using IPA. We obtained the representative signalling of OA using RNA-seq data of chondrocytes co-treated with BBC0403 and IL-1β and treated only with IL-1β as control. When BBC0403 and IL-1β were co-administered, many NF-κB and MAPK signalling genes were down-regulated, compared to using IL-1β alone (Figure 4a). These changes in gene expression are shown in heat maps (Figure 4b). Heatmaps of IL-1β-up-regulated genes showed that BBC0403 suppressed the expression of many genes related to each signalling pathway. Additionally, doughnut graphs showed that most of the IL-1β-up-regulated genes in each signalling were down-regulated (Figure 4c). Many genes related to the two signalling pathways were up-regulated by IL-1β compared with the control, but BBC0403 down-regulated many genes that IL-1β had increased. Specifically, 40 of 57 genes that IL-1β up-regulated were down-regulated by BBC0403 in p38 signalling; 61 of 99 genes in NF-κB, 34 of 64 in JNK and 64 of 110 in ERK signalling were down-regulated by BBC0403 compared with IL-1β as control.

Alterations in signalling induced by BBC0403 were confirmed *in vitro*. BBC0403 in various concentrations was used to treat mouse articular chondrocytes for 12 h, and IL-1β (1 $ng \cdot ml^{-1}$) was applied for

FIGURE 3 BBC0403 inhibited DMM surgery-induced expression of catabolic factors, preventing cartilage degradation. (a) This is an *in vivo* experimental scheme to evaluate the effect of BBC0403 on osteoarthritis (OA). DMM surgery was conducted on 12-week-old mice to make an OA mouse model. After 4 weeks after surgery, BBC0403 was intra-articular (i.a.) injected once a week for 7 weeks. (b) BBC0403 was injected with 5 and 10 $\mu g \cdot kg^{-1}$, and the histopathology of the knee joint was analysed by safranin O staining. Orange lines indicate tidemarks. (c, d) The histopathology assessments for the anti-OA effect of BBC0403 were presented using Osteoarthritis Research Society International scoring (c) and subchondral bone plate (SBP) thickness (d) ($n = 5$). (e, f) In the knee joint, the change of expression of catabolic factors after injecting BBC0403 (10 $\mu g \cdot kg^{-1}$) was analysed by immunohistochemistry (e) and quantified by ImageJ (f) ($n = 5$). Values are presented as means ± SD, assessed using one-way ANOVA with Bonferroni's test (d, f) and Kruskal–Wallis test using Dunn's (c). $^*P < 0.05$. Sham: The group without surgery; Control: the DMM-induced group with i.a. injection of PBS was the control. The cartilage and each tissue were captured under the microscope at 40×, 100× and 400×. Scale bar = 100 μm.

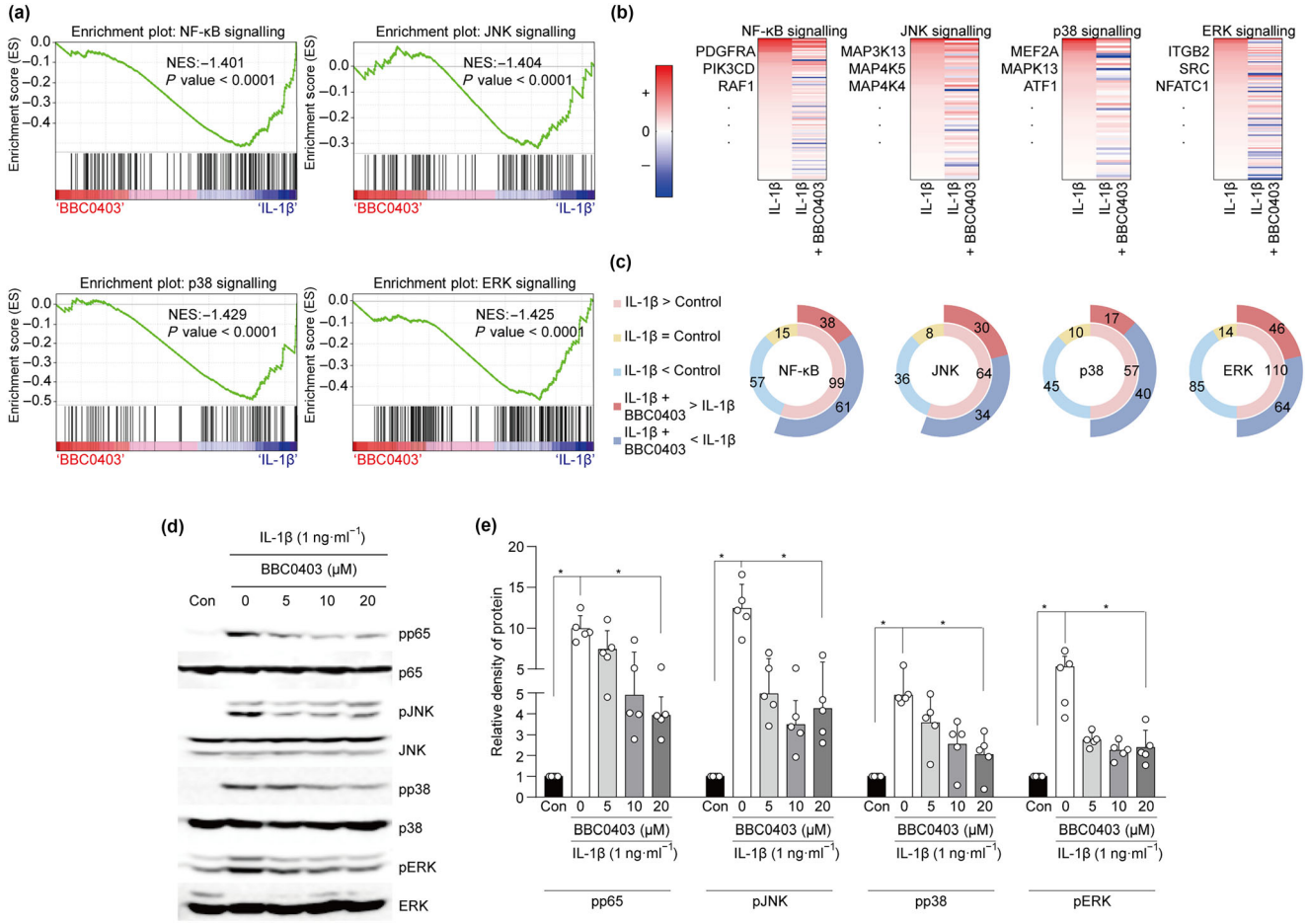

FIGURE 4 The anti-OA effect of BBC0403 is associated with inhibiting NF-κB and MAPK signalling activated by IL-1β. (a–c) RNA-seq silico analysis was performed with RNA samples isolated from three groups (control, IL-1β, IL-1β + BBC0403 20 μM). Gene set enrichment analysis (GSEA) was conducted to analyse the association with each signalling (a), and heatmaps and doughnut graphs were used to show changes in IL-1β-up-regulated gene expression caused by BBC0403 (b, c). (d, e) Mouse articular chondrocytes were treated with BBC0403 at various concentrations for 12 h, and IL-1β (1 ng·ml^{-1}) was added 10 min before harvest. Western blotting was conducted (d) to evaluate the level of each signalling and was verified by densitometry (e) ($n = 5$). Values were assessed using Kruskal–Wallis and Dunn's tests and are presented as means ± SD. *$P < 0.05$. FDR, false discovery rate; NES, normalized enrichment score. Control: The group treated with PBS was the control.

10 min before harvest. BBC0403 decreased the level of pp65 protein and increased the level of pIκB protein (Figure 4d,e). This indicates that BBC0403 suppresses IL-1β-induced NF-κB signalling. In addition, BBC0403 decreased the protein levels of pJNK, pERK and pp38 compared to those in the control group (Figure 4d,e), showing that BBC0403 suppressed MAPK signalling induced by IL-1β. BBC0403 was identified to suppress OA progression via MAPK and NF-κB signalling (Figure 5).

4 | DISCUSSION AND CONCLUSION

Articular cartilage deterioration is the primary symptom of OA, a degenerative condition causing discomfort (Yao et al., 2023). OA can only be managed and delayed at the disease management level, with no existing medication preventing or postponing its onset (Martel-Pelletier et al., 2016). I.a. injection is a cost-effective treatment for OA, but no evidence exists that hyaluronic acid and corticoids provide complete relief for OA (Jørgensen et al., 2010). Therefore, the development of novel i.a. injection drugs is necessary.

This study suggests that BBC0403 regulates MAPK and NF-κB signalling. When BBC0403 was administered with IL-1β, IL-1β-induced ERK, p38 and JNK signalling decreased. MAPK signalling affects chondrocyte alteration, such as NF-κB signalling. p38 is a member of the MAPK superfamily, and its signalling pathway is activated by phosphorylation. Moreover, p38 signalling is associated with many age-related diseases (Barnes et al., 2019; Grootaert et al., 2021; He et al., 2020). Specifically, in OA, activation of the p38 signalling pathway up-regulates the expression of MMPs, which in turn degrades type II collagen, a component of cartilage (Liao, Zhang, et al., 2020b).

Similarly, the active forms of JNK and ERK are phosphorylated to activate active protein-1 (Park et al., 2013). Many studies have shown that JNK and ERK signalling activation is associated with OA

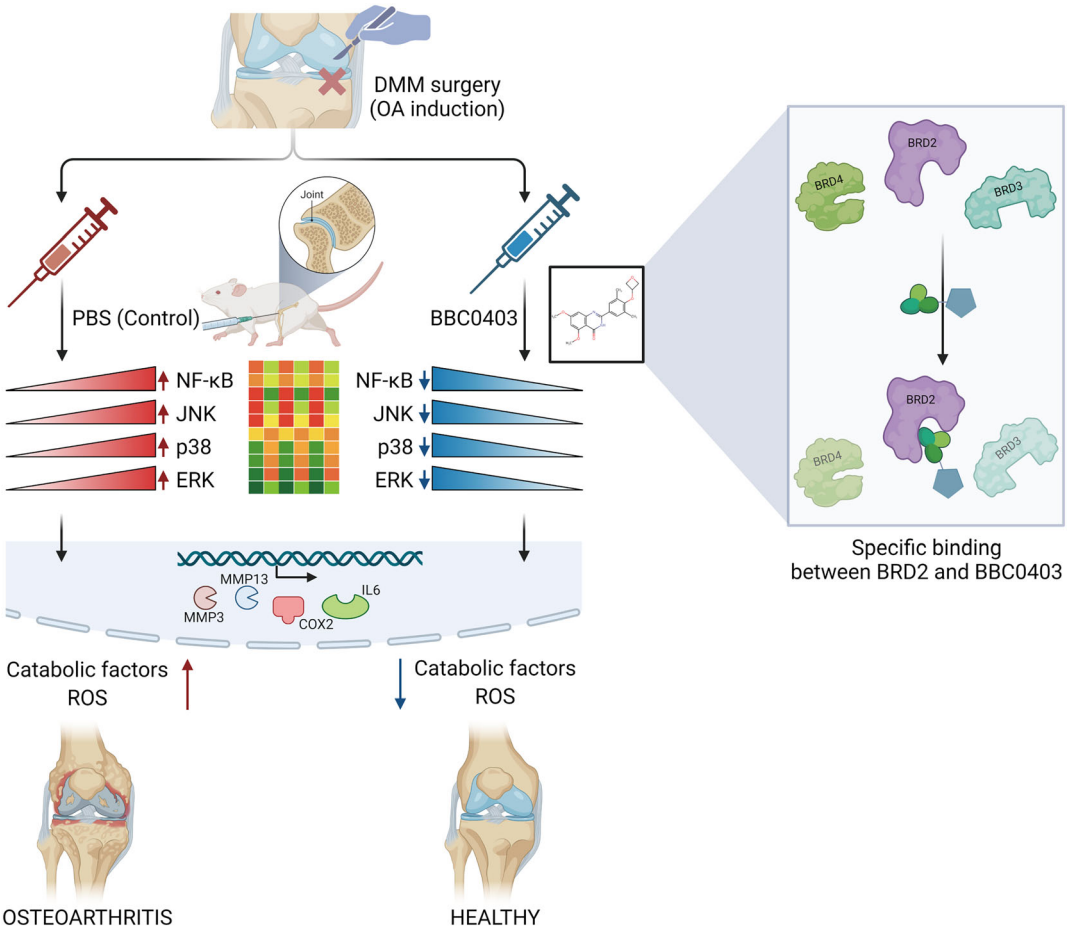

FIGURE 5 BBC0403 acquired from DNA-encoded chemical library (DEL) screening for BRD proteins showed stronger binding affinity to BRD2 than BRD3 and BRD4. In chondrocytes, BBC0403 suppressed IL-1β-induced NF-κB, ERK, JNK and p38 signalling by down-regulating the corresponding genes and decreasing the expression of Mmp3, Mmp13, Cox2 and Il-6. BBC0403 was intra-articular (i.a.) injected into the mouse knee joint after DMM surgery attenuated cartilage degradation and OA progress.

progression (Cho et al., 2023; Lin et al., 2021; Tong et al., 2019), including cell proliferation, development and other pathological processes. Yang et al. showed that chemokines, such as **CXCL8** and **CXCL11**, are increased in the synovial fluid of patients with OA and that CXCL8 and CXCL11 trigger the JNK signalling pathway, which in turn promotes apoptosis and inhibits chondrocyte proliferation (Yang et al., 2016).

ROS production significantly contributes to the onset and progression of OA. ROS are generated due to oxidative stress during cellular metabolism and can potentially harm cartilage (Deng et al., 2022; Kang et al., 2022). The 8-hydroxyguanosine (8-OHdG) biomarker is particularly noteworthy, as it signifies DNA damage and oxidative stress manifestation (Guo et al., 2016). The level of 8-OHdG is indicative of certain pathological states such as ageing, cancer and chronic kidney disease (Cavallini et al., 2007; Kondo et al., 2000; Sanchez et al., 2018). Several studies have suggested that increased levels of oxidative stress can potentially cause disturbances in the metabolic processes of chondrocytes (Kang et al., 2022). Furthermore, some studies indicated that OA pathogenesis is associated with increased 8-OHdG levels (Jeon et al., 2023; Renaudin et al., 2023).

The therapeutic potential of bromo- and extra-terminal domain inhibitors (BETis) is due to their ability to transform epigenomic DNA into small molecules. BETi binds to the bromodomains (BD1 and BD2) of BET proteins (BRD2, BRD3, BRD4 and BRDT) and inhibits their interactions with acetylated lysine residues on histone tails and transcription factors (Kulikowski et al., 2021). Although pan-BETi binds to all three BET proteins with equal affinity, selective BETi shows greater affinity for one BRD protein than the other. For example, pan-BETi JQ1 can prevent the inflammation-induced redistribution of BRD4 on chromatin, suppress the expression of inflammatory and adhesion molecules in endothelial cells induced by tumour necrosis factor-alpha, significantly reduce monocyte (THP-1 cell) adhesion to human umbilical vein endothelial cells (HUVECs) and inhibit atherogenesis in hypercholesterolaemic mice (Brown et al., 2014). However, multiple uses of pan-BET are limited by toxic effects (Doroshow et al., 2017). Therefore, it is crucial to determine whether selective BETi can maintain anti-inflammatory properties without causing toxicity. Such BETis would serve as anti-inflammatory agents in OA.

Previous research has shown that mice with low levels of BRD2 (brd2 low mice) are protected against obesity-induced inflammation

(Wang et al., 2009), indicating that BRD2 plays a critical role in regulating inflammation in response to various pro-inflammatory stimuli. Additionally, BRD2 is vital in regulating pro-inflammatory cytokines by facilitating NF-κB-regulated transcription (Belkina et al., 2013).

As previously reported, in cells treated with JQ1, the multi-target BETi, the IL-1β-induced expression of MMPs and inflammatory cytokines was reduced, and cartilage destruction was suppressed in the anterior cruciate ligament transection (ACLT) mouse model by downregulating NF-κB signalling. However, because JQ1 has a short half-life, it has not yet been evaluated in human clinical trials.

In this study, DMM surgery was chosen rather than anterior cruciate ligament transection to test the OA effects of BBC0403 in an OA C57BL/6 male mouse model. DMM surgery destabilizes the medial meniscus by transecting the medial meniscotibial ligament because of the high level of surgical expertise required and the subsequent severe OA, which may involve subchondral bone erosion, anterior cruciate ligament transection is not recommended for use in mice. DMM-induced lesions were similar in degree and location to those observed in older spontaneous mouse models of OA (Jeon et al., 2020). DMM surgery affects the chondrocyte column disarrangement of the growth plate, which does not affect cartilage destruction (Lamuedra et al., 2020). Cartilage destruction was reduced when BBC0403 was i.a. injected after DMM surgery, but chondrocyte column disarrangement was not reduced (Figure S6). A potent and specific small molecule, BETi, BBC0403, showed anti-OA effects at cellular and animal levels without organ cytotoxicity in the liver, lungs and synovium.

The classification of OA cartilage degeneration is complex because patients have various histories, symptoms and morphological changes. Common to all, however, are symptoms of pain or limitation in joint movement associated with structural joint (cartilage) damage (Aigner et al., 2015). As previously reported, increased cartilage destruction may be increasing the pain (Dai et al., 2018, 2019; Kang et al., 2022). Although we did not perform pain analysis, we speculate that BBC0403 reduced knee pain because of the inhibition of cartilage destruction. Although we demonstrated no cytotoxicity after i.a. injection, BBC0403 translation to systemic diseases still has limitations because we did not administer BBC0403 orally. Should oral administration of BBC0403 affect OA, it can be used for universal OA therapy as well as for obesity-induced inflammation regulated by BRD2 (Wang et al., 2009).

In conclusion, this study evaluated the potential of a newly developed BRD2-specific inhibitor, BBC0403, for treating OA. BBC0403 selectively targets BET proteins with a high affinity for BRD2. This selectivity enhances its efficacy while minimizing the adverse effects of OA. BBC0403 also exhibited anti-OA effects, such as suppressing catabolic factors and preventing OA cartilage degradation. Therefore, BBC0403 is a promising candidate for injectable drug therapy, specifically as a BRD2-specific inhibitor, in the treatment of OA.

AUTHOR CONTRIBUTIONS

H. Lee: Conceptualization; methodology; validation; formal analysis; investigation; writing—original draft; writing—review and editing. **J. Nam**: Validation; formal analysis. **H. Jang**: Validation; formal analysis. **Y.-S. Park**: Validation; formal analysis. **M.-H. Son**: Validation; formal analysis. **I.-H. Lee**: Validation; formal analysis; investigation; resources; writing—original draft. **S. Eyun**: Methodology. **J.-H. Yang**: Methodology. **J. Jeon**: Validation; investigation; writing—original draft. **S. Yang**: Conceptualization; investigation; resources; writing—original draft; writing—review and editing; supervision; project administration; funding acquisition. All authors have read and agreed to the published version of the manuscript.

ACKNOWLEDGEMENTS

This work was supported by the National Research Foundation, funded by the Ministry of Science & ICT (NRF-2022R1A2C2004343, RS-2023-00223552, RS-2024-00400945 and RS-2024-00335111).

CONFLICT OF INTEREST STATEMENT

The authors declare no conflict of interest.

DATA AVAILABILITY STATEMENT

The data used to support the findings of this study have been included in this article.

DECLARATION OF TRANSPARENCY AND SCIENTIFIC RIGOUR

This Declaration acknowledges that this paper adheres to the principles for transparent reporting and scientific rigour of preclinical research as stated in the *BJP* guidelines for Design and Analysis, Immunoblotting and Immunochemistry and Animal Experimentation, and as recommended by funding agencies, publishers and other organizations engaged with supporting research.

ORCID

Hyemi Lee https://orcid.org/0000-0002-7410-203X
Siyoung Yang https://orcid.org/0000-0002-6374-0140

REFERENCES

Aigner, T., Schmitz, N., & Salter, D. M. (2015). 175—Pathogenesis and pathology of osteoarthritis. In M. C. Hochberg, A. J. Silman, J. S. Smolen, M. E. Weinblatt, & M. H. Weisman (Eds.), *Rheumatology (sixth edition)* (pp. 1462–1476). Mosby. https://doi.org/10.1016/B978-0-323-09138-1.00175-3

Akhtar, N., & Haqqi, T. M. (2012). MicroRNA-199a* regulates the expression of cyclooxygenase-2 in human chondrocytes. *Annals of the Rheumatic Diseases*, *71*(6), 1073–1080. https://doi.org/10.1136/annrheumdis-2011-200519

Alexander, S. P. H., Fabbro, D., Kelly, E., Mathie, A. A., Peters, J. A., Veale, E. L., Armstrong, J. F., Faccenda, E., Harding, S. D., Davies, J. A., Beuve, A., Brouckaert, P., Bryant, C., Burnett, J. C., Farndale, R. W., Friebe, A., Garthwaite, J., Hobbs, A. J., Jarvis, G. E., … Waldman, S. A. (2023a). The Concise Guide to PHARMACOLOGY 2023/24: Catalytic receptors. *British Journal of Pharmacology*, *180*, S241–S288. https://doi.org/10.1111/bph.16180

Alexander, S. P. H., Fabbro, D., Kelly, E., Mathie, A. A., Peters, J. A., Veale, E. L., Armstrong, J. F., Faccenda, E., Harding, S. D., Davies, J. A., Annett, S., Boison, D., Burns, K. E., Dessauer, C., Gertsch, J., Helsby, N. A., Izzo, A. A., Ostrom, R., Papapetropoulos, A., …

Wong, S. S. (2023b). The Concise Guide to PHARMACOLOGY 2023/24: Enzymes. *British Journal of Pharmacology*, *180*, S289–S373. https://doi.org/10.1111/bph.16181

Alexander, S. P. H., Roberts, R. E., Broughton, B. R. S., Sobey, C. G., George, C. H., Stanford, S. C., Cirino, G., Docherty, J. R., Giembycz, M. A., Hoyer, D., Insel, P. A., Izzo, A. A., Ji, Y., MacEwan, D. J., Mangum, J., Wonnacott, S., & Ahluwalia, A. (2018). Goals and practicalities of immunoblotting and immunohistochemistry: A guide for submission to the *British Journal of Pharmacology*. *British Journal of Pharmacology*, *175*, 407–411. https://doi.org/10.1111/bph.14112

An, Q. D., Li, Y. Y., Zhang, H. X., Lu, J., Yu, X. D., Lin, Q., & Zhang, Y. G. (2018). Inhibition of bromodomain-containing protein 4 ameliorates oxidative stress-mediated apoptosis and cartilage matrix degeneration through activation of NF-E2-related factor 2-heme oxygenase-1 signaling in rat chondrocytes. *Journal of Cellular Biochemistry*, *119*(9), 7719–7728. https://doi.org/10.1002/jcb.27122

Ayhan, E., Kesmezacar, H., & Akgun, I. (2014). Intraarticular injections (corticosteroid, hyaluronic acid, platelet rich plasma) for the knee osteoarthritis. *World Journal of Orthopedics*, *5*(3), 351–361. https://doi.org/10.5312/wjo.v5.i3.351

Barnes, P. J., Baker, J., & Donnelly, L. E. (2019). Cellular senescence as a mechanism and target in chronic lung diseases. *American Journal of Respiratory and Critical Care Medicine*, *200*(5), 556–564. https://doi.org/10.1164/rccm.201810-1975TR

Belkina, A. C., Nikolajczyk, B. S., & Denis, G. V. (2013). BET protein function is required for inflammation: Brd2 genetic disruption and BET inhibitor JQ1 impair mouse macrophage inflammatory responses. *Journal of Immunology*, *190*(7), 3670–3678. https://doi.org/10.4049/jimmunol.1202838

Brown, J. D., Lin, C. Y., Duan, Q., Griffin, G., Federation, A. J., Paranal, R. M., Bair, S., Newton, G., Lichtman, A. H., Kung, A. L., Yang, T., Wang, H., Luscinskas, F. W., Croce, K. J., Bradner, J. E., & Plutzky, J. (2014). NF-κB directs dynamic super enhancer formation in inflammation and atherogenesis. *Molecular Cell*, *56*(2), 219–231. https://doi.org/10.1016/j.molcel.2014.08.024

Cavallini, G., Donati, A., Taddei, M., & Bergamini, E. (2007). Evidence for selective mitochondrial autophagy and failure in aging. *Autophagy*, *3*(1), 26–27. https://doi.org/10.4161/auto.3268

Cheung, K. L., Zhang, F., Jaganathan, A., Sharma, R., Zhang, Q., Konuma, T., Shen, T., Lee, J. Y., Ren, C., Chen, C. H., Lu, G., Olson, M. R., Zhang, W., Kaplan, M. H., Littman, D. R., Walsh, M. J., Xiong, H., Zeng, L., & Zhou, M. M. (2017). Distinct roles of Brd2 and Brd4 in potentiating the transcriptional program for Th17 cell differentiation. *Molecular Cell*, *65*(6), 1068–1080.e5. https://doi.org/10.1016/j.molcel.2016.12.022

Cho, C., Lee, J. S., Oh, H., Kang, L. J., Hwang, Y., Chae, S., Lee, I. J., Kim, S. J., Woo, H., Eyun, S. I., Kang, H. C., Choi, W. I., & Yang, S. (2022). Fructose-derived Levan nanoparticles protect against osteoarthritis by directly blocking CD44 activation. *Small*, *18*, 2202146. https://doi.org/10.1002/smll.202202146

Cho, C., Oh, H., Lee, J. S., Kang, L. J., Oh, E. J., Hwang, Y., Kim, S. J., Bae, Y. S., Kim, E. J., Kang, H. C., Choi, W. I., & Yang, S. (2023). Prussian blue nanozymes coated with Pluronic attenuate inflammatory osteoarthritis by blocking c-Jun N-terminal kinase phosphorylation. *Biomaterials*, *297*, 122131. https://doi.org/10.1016/j.biomaterials.2023.122131

Curtis, M. J., Alexander, S. P. H., Cirino, G., George, C. H., Kendall, D. A., Insel, P. A., Izzo, A. A., Ji, Y., Panettieri, R. A., Patel, H. H., Sobey, C. G., Stanford, S. C., Stanley, P., Stefanska, B., Stephens, G. J., Teixeira, M. M., Vergnolle, N., & Ahluwalia, A. (2022). Planning experiments: Updated guidance on experimental design and analysis and their reporting III. *British Journal of Pharmacology*., *179*, 3907–3913. https://doi.org/10.1111/bph.15868

da Costa, B. R., Reichenbach, S., Keller, N., Nartey, L., Wandel, S., Jüni, P., & Trelle, S. (2017). Effectiveness of non-steroidal anti-inflammatory drugs for the treatment of pain in knee and hip osteoarthritis: A network meta-analysis. *Lancet*, *390*(10090), e21–e33. https://doi.org/10.1016/s0140-6736(17)31744-0

Dai, J., Zhou, S., Ge, Q., Qin, J., Chen, D., Xu, Z., Shi, D., Li, J., Ju, H., Cao, Y., Zheng, M., Li, C. J., Gao, X., Teng, H., & Jiang, Q. (2018). Bi-directional regulation of cartilage metabolism by inhibiting BET proteins-analysis of the effect of I-BET151 on human chondrocytes and murine joints. *Journal of Orthopaedic Surgery and Research*, *13*(1), 118. https://doi.org/10.1186/s13018-018-0797-y

Dai, J., Zhou, S., Ge, Q., Qin, J., Li, J., Ju, H., Cao, Y., Zheng, M., Li, C., Gao, X., Teng, H., & Jiang, Q. (2019). Recruitment of Brd3 and Brd4 to acetylated chromatin is essential for proinflammatory cytokine-induced matrix-degrading enzyme expression. *Journal of Orthopaedic Surgery and Research*, *14*(1), 59. https://doi.org/10.1186/s13018-019-1091-3

Deng, C., Zhou, Q., Zhang, M., Li, T., Chen, H., Xu, C., Feng, Q., Wang, X., Yin, F., Cheng, Y., & Wu, C. (2022). Bioceramic scaffolds with antioxidative functions for ROS scavenging and osteochondral regeneration. *Advancement of Science*, *9*(12), e2105727. https://doi.org/10.1002/advs.202105727

Devaiah, B. N., Case-Borden, C., Gegonne, A., Hsu, C. H., Chen, Q., Meerzaman, D., Dey, A., Ozato, K., & Singer, D. S. (2016). BRD4 is a histone acetyltransferase that evicts nucleosomes from chromatin. *Nature Structural & Molecular Biology*, *23*(6), 540–548. https://doi.org/10.1038/nsmb.3228

Dong, X., Hu, X., Chen, J., Hu, D., & Chen, L. F. (2018). BRD4 regulates cellular senescence in gastric cancer cells via E2F/miR-106b/p21 axis. *Cell Death & Disease*, *9*(2), 203. https://doi.org/10.1038/s41419-017-0181-6

Doroshow, D. B., Eder, J. P., & LoRusso, P. M. (2017). BET inhibitors: A novel epigenetic approach. *Annals of Oncology*, *28*(8), 1776–1787. https://doi.org/10.1093/annonc/mdx157

Fu, L. L., Tian, M., Li, X., Li, J. J., Huang, J., Ouyang, L., Zhang, Y., & Liu, B. (2015). Inhibition of BET bromodomains as a therapeutic strategy for cancer drug discovery. *Oncotarget*, *6*(8), 5501–5516. https://doi.org/10.18632/oncotarget.3551

Fukui, T., Yik, J. H. N., Doyran, B., Davis, J., Haudenschild, A. K., Adamopoulos, I. E., Han, L., & Haudenschild, D. R. (2021). Bromodomain-containing-protein-4 and cyclin-dependent-kinase-9 inhibitors interact synergistically in vitro and combined treatment reduces post-traumatic osteoarthritis severity in mice. *Osteoarthritis and Cartilage*, *29*(1), 68–77. https://doi.org/10.1016/j.joca.2020.07.012

Gilan, O., Rioja, I., Knezevic, K., Bell, M. J., Yeung, M. M., Harker, N. R., Lam, E. Y. N., Chung, C. W., Bamborough, P., Petretich, M., Urh, M., Atkinson, S. J., Bassil, A. K., Roberts, E. J., Vassiliadis, D., Burr, M. L., Preston, A. G. S., Wellaway, C., Werner, T., … Dawson, M. A. (2020). Selective targeting of BD1 and BD2 of the BET proteins in cancer and immunoinflammation. *Science*, *368*(6489), 387–394. https://doi.org/10.1126/science.aaz8455

Glasson, S. S., Blanchet, T. J., & Morris, E. A. (2007). The surgical destabilization of the medial meniscus (DMM) model of osteoarthritis in the 129/SvEv mouse. *Osteoarthritis and Cartilage*, *15*(9), 1061–1069. https://doi.org/10.1016/j.joca.2007.03.006

Glasson, S. S., Chambers, M. G., van den Berg, W. B., & Little, C. B. (2010). The OARSI histopathology initiative—Recommendations for histological assessments of osteoarthritis in the mouse. *Osteoarthritis and Cartilage*, *18*(Suppl 3), S17–S23. https://doi.org/10.1016/j.joca.2010.05.025

Grootaert, M. O. J., Finigan, A., Figg, N. L., Uryga, A. K., & Bennett, M. R. (2021). SIRT6 protects smooth muscle cells from senescence and

reduces atherosclerosis. *Circulation Research*, *128*(4), 474–491. https://doi.org/10.1161/circresaha.120.318353

Guo, Z., Liu, X., Liu, Y., Wu, G., & Lu, X. (2016). Constructing a novel 8-hydroxy-2′-deoxyguanosine electrochemical sensor and application in evaluating the oxidative damages of DNA and guanine. *Biosensors & Bioelectronics*, *86*, 671–676. https://doi.org/10.1016/j.bios.2016.07.033

He, D., Wu, H., Xiang, J., Ruan, X., Peng, P., Ruan, Y., Chen, Y. G., Wang, Y., Yu, Q., Zhang, H., Habib, S. L., de Pinho, R. A., Liu, H., & Li, B. (2020). Gut stem cell aging is driven by mTORC1 via a p38 MAPK-p53 pathway. *Nature Communications*, *11*(1), 37. https://doi.org/10.1038/s41467-019-13911-x

Jeon, J., Lee, H., Jeon, M. S., Kim, S. J., Choi, C., Kim, K. W., Yang, D. J., Lee, S., Bae, Y. S., Choi, W. I., Jung, J., Eyun, S. I., & Yang, S. (2023). Blockade of activin receptor IIB protects arthritis pathogenesis by non-amplification of activin A-ACVR2B-NOX4 axis pathway. *Advancement of Science*, *10*(14), e2205161. https://doi.org/10.1002/advs.202205161

Jeon, J., Noh, H. J., Lee, H., Park, H. H., Ha, Y. J., Park, S. H., Lee, H., Kim, S. J., Kang, H. C., Eyun, S. I., Yang, S., & Kim, Y. S. (2020). TRIM24-RIP3 axis perturbation accelerates osteoarthritis pathogenesis. *Annals of the Rheumatic Diseases*, *79*(12), 1635–1643. https://doi.org/10.1136/annrheumdis-2020-217904

Jiang, Y., Zhu, L., Zhang, T., Lu, H., Wang, C., Xue, B., Xu, X., Liu, Y., Cai, Z., Sang, W., Hua, Y., & Ma, J. (2017). BRD4 has dual effects on the HMGB1 and NF-κB signaling pathways and is a potential therapeutic target for osteoarthritis. *Biochimica et Biophysica Acta - Molecular Basis of Disease*, *1863*(12), 3001–3015. https://doi.org/10.1016/j.bbadis.2017.08.009

Jørgensen, A., Stengaard-Pedersen, K., Simonsen, O., Pfeiffer-Jensen, M., Eriksen, C., Bliddal, H., Pedersen, N. W., Bødtker, S., Hørslev-Petersen, K., Snerum, L. Ø., Egund, N., & Frimer-Larsen, H. (2010). Intra-articular hyaluronan is without clinical effect in knee osteoarthritis: A multicentre, randomised, placebo-controlled, double-blind study of 337 patients followed for 1 year. *Annals of the Rheumatic Diseases*, *69*(6), 1097–1102. https://doi.org/10.1136/ard.2009.118042

Kang, D., Lee, J., Jung, J., Carlson, B. A., Chang, M. J., Chang, C. B., Kang, S. B., Lee, B. C., Gladyshev, V. N., Hatfield, D. L., Lee, B. J., & Kim, J. H. (2022). Selenophosphate synthetase 1 deficiency exacerbates osteoarthritis by dysregulating redox homeostasis. *Nature Communications*, *13*(1), 779. https://doi.org/10.1038/s41467-022-28385-7

Kang, J. H., Splinter, P. L., Trussoni, C. E., Pirius, N. E., Gores, G. J., LaRusso, N. F., & O'Hara, S. P. (2023). The epigenetic reader, bromodomain containing 2, mediates cholangiocyte senescence via interaction with ETS proto-oncogene 1. *Gastroenterology*, *165*, 228–243.e2. https://doi.org/10.1053/j.gastro.2023.03.235

Kapoor, M., Martel-Pelletier, J., Lajeunesse, D., Pelletier, J. P., & Fahmi, H. (2011). Role of proinflammatory cytokines in the pathophysiology of osteoarthritis. *Nature Reviews Rheumatology*, *7*(1), 33–42. https://doi.org/10.1038/nrrheum.2010.196

Kiani, A. K., Pheby, D., Henehan, G., Brown, R., Sieving, P., Sykora, P., Marks, R., Falsini, B., Capodicasa, N., Miertus, S., Lorusso, L., Dondossola, D., Tartaglia, G. M., Ergoren, M. C., Dundar, M., Michelini, S., Malacarne, D., Bonetti, G., Dautaj, A., … INTERNATIONAL BIOETHICS STUDY GROUP. (2022). Ethical considerations regarding animal experimentation. *Journal of Preventive Medicine and Hygiene*, *63*(2 Suppl 3), E255–E266. https://doi.org/10.15167/2421-4248/jpmh2022.63.2S3.2768

Kohandani, F., Jazireian, P., Favaedi, R., Sadighi Gilani, M. A., Moshtaghioun, S. M., & Shahhoseini, M. (2022). Epigenetic dysregulation of BRDT gene in testis tissues of infertile men: Case-control study. *Cell Journal*, *24*(2), 99–102. https://doi.org/10.22074/cellj.2022.7724

Kondo, S., Toyokuni, S., Tanaka, T., Hiai, H., Onodera, H., Kasai, H., & Imamura, M. (2000). Overexpression of the hOGG1 gene and high 8-hydroxy-2′-deoxyguanosine (8-OHdG) lyase activity in human colorectal carcinoma: Regulation mechanism of the 8-OHdG level in DNA. *Clinical Cancer Research*, *6*(4), 1394–1400.

Kulikowski, E., Rakai, B. D., & Wong, N. C. W. (2021). Inhibitors of bromodomain and extra-terminal proteins for treating multiple human diseases. *Medicinal Research Reviews*, *41*(1), 223–245. https://doi.org/10.1002/med.21730

Kuyinu, E. L., Narayanan, G., Nair, L. S., & Laurencin, C. T. (2016). Animal models of osteoarthritis: Classification, update, and measurement of outcomes. *Journal of Orthopaedic Surgery and Research*, *11*, 19. https://doi.org/10.1186/s13018-016-0346-5

Lamuedra, A., Gratal, P., Calatrava, L., Ruiz-Perez, V. L., Largo, R., & Herrero-Beaumont, G. (2020). Disorganization of chondrocyte columns in the growth plate does not aggravate experimental osteoarthritis in mice. *Scientific Reports*, *10*(1), 10745. https://doi.org/10.1038/s41598-020-67518-0

Lee, H., Jang, D., Jeon, J., Cho, C., Choi, S., Han, S. J., Oh, E., Nam, J., Park, C. H., Shin, Y. S., Yun, S. P., Yang, S., & Kang, L. J. (2020). Seomae mugwort and jaceosidin attenuate osteoarthritic cartilage damage by blocking IκB degradation in mice. *Journal of Cellular and Molecular Medicine*, *24*(14), 8126–8137. https://doi.org/10.1111/jcmm.15471

Leong, X. F., Ng, C. Y., & Jaarin, K. (2015). Animal models in cardiovascular research: Hypertension and atherosclerosis. *BioMed Research International*, *2015*, 528757. https://doi.org/10.1155/2015/528757

Li, X., Dai, B., Guo, J., Zheng, L., Guo, Q., Peng, J., Xu, J., & Qin, L. (2021). Nanoparticle-cartilage interaction: Pathology-based intra-articular drug delivery for osteoarthritis therapy. *Nanomicro Lett*, *13*(1), 149. https://doi.org/10.1007/s40820-021-00670-y

Li, Y., Xie, W., Xiao, W., & Dou, D. (2022). Progress in osteoarthritis research by the National Natural Science Foundation of China. *Bone Research*, *10*(1), 41. https://doi.org/10.1038/s41413-022-00207-y

Liao, C. R., Wang, S. N., Zhu, S. Y., Wang, Y. Q., Li, Z. Z., Liu, Z. Y., Jiang, W. S., Chen, J. T., & Wu, Q. (2020a). Advanced oxidation protein products increase TNF-α and IL-1β expression in chondrocytes via NADPH oxidase 4 and accelerate cartilage degeneration in osteoarthritis progression. *Redox Biology*, *28*, 101306. https://doi.org/10.1016/j.redox.2019.101306

Liao, L., Zhang, S., Zhao, L., Chang, X., Han, L., Huang, J., & Chen, D. (2020b). Acute synovitis after trauma precedes and is associated with osteoarthritis onset and progression. *International Journal of Biological Sciences*, *16*(6), 970–980. https://doi.org/10.7150/ijbs.39015

Lilley, E., Stanford, S. C., Kendall, D. E., Alexander, S. P., Cirino, G., Docherty, J. R., George, C. H., Insel, P. A., Izzo, A. A., Ji, Y., Panettieri, R. A., Sobey, C. G., Stefanska, B., Stephens, G., Teixeira, M., & Ahluwalia, A. (2020). ARRIVE 2.0 and the *British Journal of Pharmacology*: Updated guidance for 2020. *British Journal of Pharmacology*, *177*, 3611–3616. https://doi.org/10.1111/bph.15178

Lin, Z., Miao, J., Zhang, T., He, M., Wang, Z., Feng, X., & Bai, L. (2021). JUNB-FBXO21-ERK axis promotes cartilage degeneration in osteoarthritis by inhibiting autophagy. *Aging Cell*, *20*(2), e13306. https://doi.org/10.1111/ace

Lockwood, W. W., Zejnullahu, K., Bradner, J. E., & Varmus, H. (2012). Sensitivity of human lung adenocarcinoma cell lines to targeted inhibition of BET epigenetic signaling proteins. *Proceedings of the National Academy of Sciences of the United States of America*, *109*(47), 19408–19413. https://doi.org/10.1073/pnas.1216363109l.13306

Lovén, J., Hoke, H. A., Lau, A., Orlando, D. A., Vakoc, C. R., Bradner, J. E., Lee, T. I., & Young, R. A. (2013). Selective inhibition of tumor

oncogenes by disruption of super-enhancers. *Cell*, *153*(2), 320–334. https://doi.org/10.1016/j.cell.2013.03.036

Ma, H. L., Blanchet, T. J., Peluso, D., Hopkins, B., Morris, E. A., & Glasson, S. S. (2007). Osteoarthritis severity is sex dependent in a surgical mouse model. *Osteoarthritis and Cartilage*, *15*(6), 695–700. https://doi.org/10.1016/j.joca.2006.11.005

Martel-Pelletier, J., Barr, A. J., Cicuttini, F. M., Conaghan, P. G., Cooper, C., Goldring, M. B., Goldring, S. R., Jones, G., Teichtahl, A. J., & Pelletier, J. P. (2016). Osteoarthritis. *Nature Reviews Disease Primers*, *2*(1), 16072. https://doi.org/10.1038/nrdp.2016.72

McGettigan, P., & Henry, D. (2013). Use of non-steroidal anti-inflammatory drugs that elevate cardiovascular risk: An examination of sales and essential medicines lists in low-, middle-, and high-income countries. *PLoS Medicine*, *10*(2), e1001388. https://doi.org/10.1371/journal.pmed.1001388

Miyamoto, S., Nakamura, J., Orita, S., Omae, T., Nakajima, T., Suzuki, T., & Takahashi, K. (2016). Intra-articular injection of mono-iodoacetate induces osteoarthritis of the hip in rats. *BMC Musculoskeletal Disorders*, *17*, 132. https://doi.org/10.1186/s12891-016-0985-z

Modukuri, R. K., Yu, Z., Tan, Z., Ta, H. M., Ucisik, M. N., Jin, Z., Anglin, J. L., Sharma, K. L., Nyshadham, P., Li, F., Riehle, K., Faver, J. C., Duong, K., Nagarajan, S., Simmons, N., Palmer, S. S., Teng, M., Young, D. W., Yi, J. S., … Matzuk, M. M. (2022). Discovery of potent BET bromodomain 1 stereoselective inhibitors using DNA-encoded chemical library selections. *Proceedings of the National Academy of Sciences of the United States of America*, *119*(22), e2122506119. https://doi.org/10.1073/pnas.2122506119

Nagira, K., Ikuta, Y., Shinohara, M., Sanada, Y., Omoto, T., Kanaya, H., Nakasa, T., Ishikawa, M., Adachi, N., Miyaki, S., & Lotz, M. (2020). Histological scoring system for subchondral bone changes in murine models of joint aging and osteoarthritis. *Scientific Reports*, *10*(1), 10077. https://doi.org/10.1038/s41598-020-66979-7

Ott, C. J., Kopp, N., Bird, L., Paranal, R. M., Qi, J., Bowman, T., Rodig, S. J., Kung, A. L., Bradner, J. E., & Weinstock, D. M. (2012). BET bromodomain inhibition targets both c-Myc and IL7R in high-risk acute lymphoblastic leukemia. *Blood*, *120*(14), 2843–2852. https://doi.org/10.1182/blood-2012-02-413021

Park, J. E., Yuen, H. F., Zhou, J. B., al-aidaroos, A. Q. O., Guo, K., Valk, P. J., Zhang, S. D., Chng, W. J., Hong, C. W., Mills, K., & Zeng, Q. (2013). Oncogenic roles of PRL-3 in FLT3-ITD induced acute myeloid leukaemia. *EMBO Molecular Medicine*, *5*(9), 1351–1366. https://doi.org/10.1002/emmm.201202183

Percie du Sert, N., Hurst, V., Ahluwalia, A., Alam, S., Avey, M. T., Baker, M., Browne, W. J., Clark, A., Cuthill, I. C., Dirnagl, U., Emerson, M., Garner, P., Holgate, S. T., Howells, D. W., Karp, N. A., Lazic, S. E., Lidster, K., MacCallum, C. J., Macleod, M., … Würbel, H. (2020). The ARRIVE guidelines 2.0: Updated guidelines for reporting animal research. *PLoS Biology*, *18*(7), e3000410. https://doi.org/10.1371/journal.pbio.3000410

Pinz, S., Unser, S., Buob, D., Fischer, P., Jobst, B., & Rascle, A. (2015). Deacetylase inhibitors repress STAT5-mediated transcription by interfering with bromodomain and extra-terminal (BET) protein function. *Nucleic Acids Research*, *43*(7), 3524–3545. https://doi.org/10.1093/nar/gkv188

Renaudin, F., Oudina, K., Gerbaix, M., McGilligan Subilia, M., Paccaud, J., Jaquet, V., Krause, K. H., Ferrari, S., Laumonier, T., & Hannouche, D. (2023). NADPH oxidase 4 deficiency attenuates experimental osteoarthritis in mice. *RMD Open*, *9*(1), e002856. https://doi.org/10.1136/rmdopen-2022-002856

Sampath, S. J. P., Kotikalapudi, N., & Venkatesan, V. (2021). A novel therapeutic combination of mesenchymal stem cells and stigmasterol to attenuate osteoarthritis in rodent model system—A proof of concept study. *Stem Cell Investigation*, *8*, 5. https://doi.org/10.21037/sci-2020-048

Sanchez, M., Roussel, R., Hadjadj, S., Moutairou, A., Marre, M., Velho, G., & Mohammedi, K. (2018). Plasma concentrations of 8-hydroxy-2′-deoxyguanosine and risk of kidney disease and death in individuals with type 1 diabetes. *Diabetologia*, *61*(4), 977–984. https://doi.org/10.1007/s00125-017-4510-1

Sato, H., Sato, S., Wang, Y. M., & Horikoshi, I. (1996). Add-in macros for rapid and versatile calculation of non-compartmental pharmacokinetic parameters on Microsoft Excel spreadsheets. *Computer Methods and Programs in Biomedicine*, *50*(1), 43–52. https://doi.org/10.1016/0169-2607(96)01730-0

Shahbazi, J., Liu, P. Y., Atmadibrata, B., Bradner, J. E., Marshall, G. M., Lock, R. B., & Liu, T. (2016). The bromodomain inhibitor JQ1 and the histone deacetylase inhibitor panobinostat synergistically reduce N-Myc expression and induce anticancer effects. *Clinical Cancer Research: An Official Journal of the American Association for Cancer Research*, *22*(10), 2534–2544. https://doi.org/10.1158/1078-0432.CCR-15-1666

Shang, E., Wang, X., Wen, D., Greenberg, D. A., & Wolgemuth, D. J. (2009). Double bromodomain-containing gene Brd2 is essential for embryonic development in mouse. *Developmental Dynamics*, *238*(4), 908–917. https://doi.org/10.1002/dvdy.21911

Shu, S., Wu, H. J., Ge, J. Y., Zeid, R., Harris, I. S., Jovanović, B., Murphy, K., Wang, B., Qiu, X., Endress, J. E., Reyes, J., Lim, K., Font-Tello, A., Syamala, S., Xiao, T., Reddy Chilamakuri, C. S., Papachristou, E. K., D'Santos, C., Anand, J., … Polyak, K. (2020). Synthetic lethal and resistance interactions with BET bromodomain inhibitors in triple-negative breast cancer. *Molecular Cell*, *78*(6), 1096–1113.e1098. https://doi.org/10.1016/j.molcel.2020.04.027

Tong, W., Zeng, Y., Chow, D. H. K., Yeung, W., Xu, J., Deng, Y., Chen, S., Zhao, H., Zhang, X., Ho, K. K., Qin, L., & Mak, K. K. L. (2019). Wnt16 attenuates osteoarthritis progression through a PCP/JNK-mTORC1-PTHrP cascade. *Annals of the Rheumatic Diseases*, *78*(4), 551–561. https://doi.org/10.1136/annrheumdis-2018-214200

van der Poel, C., Levinger, P., Tonkin, B. A., Levinger, I., & Walsh, N. C. (2016). Impaired muscle function in a mouse surgical model of post-traumatic osteoarthritis. *Osteoarthritis and Cartilage*, *24*(6), 1047–1053. https://doi.org/10.1016/j.joca.2015.12.008

Wang, F., Liu, H., Blanton, W. P., Belkina, A., Lebrasseur, N. K., & Denis, G. V. (2009). Brd2 disruption in mice causes severe obesity without type 2 diabetes. *The Biochemical Journal*, *425*(1), 71–83. https://doi.org/10.1042/bj20090928

Wang, N., Wu, R., Tang, D., & Kang, R. (2021a). The BET family in immunity and disease. *Signal Transduction and Targeted Therapy*, *6*(1), 23. https://doi.org/10.1038/s41392-020-00384-4

Wang, Y., Shen, N., Li, S., Yu, H., Wang, Y., Liu, Z., Han, L., & Tang, Z. (2021b). Synergistic therapy for cervical cancer by codelivery of cisplatin and JQ1 inhibiting Plk1-mutant Trp53 Axis. *Nano Letters*, *21*(6), 2412–2421. https://doi.org/10.1021/acs.nanolett.0c04402

Yang, H., Wei, L., Yang, A., & You, H. (2021). BRD4: An emerging prospective therapeutic target in glioma. *Molecular Therapy - Oncolytics*, *21*, 1–14. https://doi.org/10.1016/j.omto.2021.03.005

Yang, P., Tan, J., Yuan, Z., Meng, G., Bi, L., & Liu, J. (2016). Expression profile of cytokines and chemokines in osteoarthritis patients: Proinflammatory roles for CXCL8 and CXCL11 to chondrocytes. *International Immunopharmacology*, *40*, 16–23. https://doi.org/10.1016/j.intimp.2016.08.005

Yao, Q., Wu, X., Tao, C., Gong, W., Chen, M., Qu, M., Zhong, Y., He, T., Chen, S., & Xiao, G. (2023). Osteoarthritis: Pathogenic signaling pathways and therapeutic targets. *Signal Transduction and Targeted Therapy*, *8*(1), 56. https://doi.org/10.1038/s41392-023-01330-w

Yoo, H. J., Choi, D. W., Roh, Y. J., Lee, Y. M., Lim, J. H., Eo, S., Lee, H. J., Kim, N. Y., Kim, S., Cho, S., Im, G., Lee, B. C., & Kim, J. H. (2022). MsrB1-regulated GAPDH oxidation plays programmatic roles in shaping metabolic and inflammatory signatures during macrophage

activation. *Cell Reports*, *41*(6), 111598. https://doi.org/10.1016/j.celrep.2022.111598

Zhang, W., Robertson, W. B., Zhao, J., Chen, W., & Xu, J. (2019). Emerging trend in the pharmacotherapy of osteoarthritis. *Frontiers in Endocrinology*, *10*, 431. https://doi.org/10.3389/fendo.2019.00431

SUPPORTING INFORMATION

Additional supporting information can be found online in the Supporting Information section at the end of this article.

How to cite this article: Lee, H., Nam, J., Jang, H., Park, Y.-S., Son, M.-H., Lee, I.-H., Eyun, S., Yang, J.-H., Jeon, J., & Yang, S. (2024). BRD2-specific inhibitor, BBC0403, inhibits the progression of osteoarthritis pathogenesis in osteoarthritis-induced C57BL/6 male mice. *British Journal of Pharmacology*, *181*(15), 2528–2544. https://doi.org/10.1111/bph.16359